

Article

# Ammonium Salts Catalyzed Acetalization Reactions in Green Ethereal Solvents

Ugo Azzena <sup>1,\*</sup>, Massimo Carraro <sup>1,2</sup>, Martina Corrias <sup>1</sup>, Rosella Crisafulli <sup>1</sup>, Lidia De Luca <sup>1</sup>, Silvia Gaspa <sup>1</sup>, Luca Nuvoli <sup>1</sup>, Salvatore Pintus <sup>1</sup>, Luisa Pisano <sup>1</sup>, Riccardo Polese <sup>1</sup>, Michela Sanna <sup>1</sup>, Giuseppe Satta <sup>1</sup>, Nina Senes <sup>1</sup>, Luigi Urtis <sup>1</sup> and Sebastiano Garroni <sup>1,\*</sup>

<sup>1</sup> Dipartimento di Chimica e Farmacia, Università di Sassari, via Vienna 2, I-07100 Sassari, Italy; mcarraro@uniss.it (M.C.); martinacorrias@tiscali.it (M.C.); ros.crisa5@gmail.com (R.C.); ldeluca@uniss.it (L.D.L.); sgaspa@uniss.it (S.G.); lucanuvoli89@gmail.com (L.N.); salvatore.pintus91@hotmail.it (S.P.); luisa@uniss.it (L.P.); riccardopolese4@gmail.com (R.P.); michela.s22@hotmail.it (M.S.); g.satta@studenti.uniss.it (G.S.); senes.nina@gmail.com (N.S.); urtis.lu@tiscali.it (L.U.)

<sup>2</sup> Consorzio Interuniversitario Reattività Chimica e Catalisi (CIRCC), via Ulpiani 27, I-70126 Bari, Italy

\* Correspondence: ugo@uniss.it (U.A.); sgarroni@uniss.it (S.G.)

Received: 31 July 2020; Accepted: 21 September 2020; Published: 24 September 2020



**Abstract:** Cyclopentyl methyl ether and 2-methyltetrahydrofuran, low impact ethereal solvents forming a positive azeotrope with water, were successfully employed as solvents in the synthesis of a variety of acetals carried out under Dean–Stark conditions in the presence of heterogeneous acidic catalysts. Under these conditions, ammonium salts, either as such or supported on SiO<sub>2</sub>, performed better or equally well than widely employed homogeneous and heterogeneous acidic catalysts such as *p*-toluenesulfonic acid, Amberlyst 15<sup>®</sup>, or Montmorillonite K10. Several examples highlight the advantage of tuning the relative acidities of ammonium salts by appropriately selecting the counterion. Within one of these examples, our protocol clearly outweighs the classic *p*-toluenesulfonic acid/toluene protocol in terms of chemoselectivity. Silica-supported catalysts were characterized by SEM, TEM, and FTIR spectroscopies, as well as by N<sub>2</sub> physisorption. Such a characterization reveals an even distribution of ammonium salts on silica, thus confirming the formation of expected catalytic supports.

**Keywords:** heterogeneous catalysis; green solvents; acetals; ammonium salts; characterization of heterogeneous catalysts

## 1. Introduction

The setup of widely employed reactions under economical, practical, and environmentally friendly conditions is a challenge of wide interest in contemporary organic chemistry. From this point of view, great attention should be dedicated to the appropriate choice of solvents as they represent one of the major contributions to the environmental impact of fine chemical synthesis [1–6].

Acetals are widely employed in multistep organic synthesis for the protection of carbonyl compounds towards basic and nucleophilic reagents, due to their general stability to a wide range of reagents and ease of removal. Additionally, they have found application in everyday life as fragrances or profragrances [7–9].

Whilst a lot of work has been devoted to the search of low impact, heterogeneous, and recyclable catalysts to promote these reactions [10–18], much less attention has been dedicated to their employment in low impact solvents. Indeed, acid-catalyzed acetalization reactions are usually run under Dean–Stark conditions employing environmentally problematic hydrocarbon solvents, such as toluene or benzene [19].

Starting from these premises and following our interest in the development of reaction procedures in environmentally friendly solvents [20–23], we investigated the acetalization of aldehydes and ketones in well-known low impact ethereal solvents forming positive azeotropes with H<sub>2</sub>O (Table 1), i.e., cyclopentyl methyl ether (CPME) [24–27] and 2-methyltetrahydrofuran (2-MeTHF) [28–31].

**Table 1.** Boiling points and percent composition of some organic solvent/H<sub>2</sub>O azeotropes.

Organic Solvent	Bp (°C)	Composition (%) <sup>1</sup>
Toluene	85.0 <sup>2</sup>	79.8:20.2 <sup>2</sup>
Benzene	69.4 <sup>2</sup>	91.1:8.9 <sup>2</sup>
CPME	83 <sup>3</sup>	83.7:16.3 <sup>3</sup>
2-MeTHF	71 <sup>4</sup>	89.4:10.6 <sup>4</sup>

<sup>1</sup> Organic solvent/H<sub>2</sub>O; w/w; <sup>2</sup> reference [32]; <sup>3</sup> reference [24]; <sup>4</sup> reference [31].

Besides being endowed with a relatively high stability towards acids and bases, both CPME and 2-MeTHF are characterized by low toxicity [33,34], relatively high boiling points, a narrow explosion range, hydrophobicity, easy drying and recovery, and appear as versatile green alternatives to ethereal solvents such as tetrahydrofuran, diethyl ether, or *tert*-butyl methyl ether. Additionally, CPME is produced via a 100% atom economical reaction [24], whilst 2-MeTHF is accessible from renewable resources [31].

In the meantime, we investigated the employment of ammonium salts and silica-supported ammonium salts as cheap, easily available, heterogeneous, and relatively mild acidic catalysts to promote the acetalization reaction. Moreover, ammonium salts offer the opportunity to evaluate how their catalytic activities vary as the counter ions change.

A preliminary communication concerning the protection of aldehydes and ketones under the abovementioned conditions has already been reported [22].

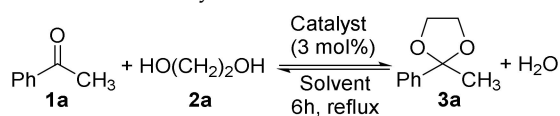
## 2. Results and Discussion

### 2.1. Synthesis of Acetals of Aldehydes and Ketones

As already reported in our previous communication [22], the reaction of acetophenone, **1a**, with an excess (1.1 to 2.0 equivalent) of 1,2-ethandiol, **2a**, was taken as a model reaction to evaluate the effectiveness of the combination of different solvents with ammonium salts as heterogeneous acidic catalysts. For comparison purposes, few reactions were run with a homogeneous acidic catalyst, i.e., *para*-toluenesulfonic acid (*p*-TSA), or with two widely employed, commercially available, heterogeneous acidic catalysts, i.e., Amberlyst 15<sup>®</sup> and Montmorillonite K10 (Mont K10).

Reactions were run by refluxing a 4 M solution of the ketone with **2a** (1.1 to 2.0 equivalent), under Dean–Stark conditions in the presence of the acidic catalysts (3 mol% relative to **1a**). Recovered reaction mixtures were very simply elaborated by filtering the catalyst followed by evaporation of the solvent in vacuo. Indeed, at variance with what was reported in our earlier communication [5c], we carefully checked that no neutralization of the reaction mixture was needed during the work-up procedure. However, the reactions run in the presence of the higher amounts of **2a** (1.5–2.0 equivalent) were additionally purified by aqueous work-up.

Our results, summarized in Table 2, show that by employing CPME as a solvent in the presence of a minimal excess of **2a** (1.1 equivalent), conversions ranging from 63% to 79% were obtained by performing reactions in the presence of different ammonium halides (Table 2, entries 1 and 2), or with glycine hydrochloride (HCl.Gly, Table 2, entry 3) [35], whilst a less satisfactory result was obtained by performing the reaction in the presence of (NH<sub>4</sub>)<sub>2</sub>SO<sub>4</sub> (Table 2, entry 4).

Table 2. Synthesis of dioxolane **3a**<sup>1</sup>.

Entry	2a (Equivalent)	Solvent	Catalyst	Product Distribution 1a/3a (%) <sup>2</sup>
1	1.1	CPME	NH <sub>4</sub> Cl	35/65 <sup>3</sup>
2	1.1	CPME	NH <sub>4</sub> Br	21/79 <sup>3</sup>
3	1.1	CPME	HCl.Gly	36/64 <sup>3</sup>
4	1.1	CPME	(NH <sub>4</sub> ) <sub>2</sub> SO <sub>4</sub>	68/32
5	1.1	CPME	(NH <sub>4</sub> )HSO <sub>4</sub>	10/90 <sup>4</sup>
6	1.5	CPME	(NH <sub>4</sub> )HSO <sub>4</sub>	5/95
7	2.0	CPME	(NH <sub>4</sub> )HSO <sub>4</sub>	<5/>95 <sup>3,5</sup>
8	2.0	Toluene	(NH <sub>4</sub> )HSO <sub>4</sub>	20/80
9	1.1	CPME	<i>p</i> -TSA	13/87
10	2.0	CPME	<i>p</i> -TSA	<5/>95
11	1.1	CPME	Amberlyst 15 <sup>®</sup>	10/90 <sup>6</sup>
12	1.1	CPME	Mont K10 <sup>7</sup>	46/54
13	1.1	2-MeTHF	(NH <sub>4</sub> )HSO <sub>4</sub>	60/40
14	2.0	2-MeTHF	(NH <sub>4</sub> )HSO <sub>4</sub>	37/63 <sup>5</sup>
15	1.1	2-MeTHF	Amberlyst 15 <sup>®</sup>	89/11 <sup>6</sup>
16	1.1	2-MeTHF	Mont K10 <sup>7</sup>	72/28

<sup>1</sup> All reactions were run at reflux for 6 h in the presence of 3 mol% of the catalyst, unless otherwise indicated; <sup>2</sup> Determined by <sup>1</sup>H-NMR analyses of crude reaction mixtures; no other reaction products were detected, unless otherwise indicated; <sup>3</sup> Comparable results were obtained recycling the recovered catalyst twice; <sup>4</sup> Comparable results were obtained when recycling the recovered catalyst four times; <sup>5</sup> Comparable results were obtained when recycling the solvent; <sup>6</sup> Unidentified by-products also formed; <sup>7</sup> 3% *w/w*.

Better results were obtained in the presence of NH<sub>4</sub>HSO<sub>4</sub> (Table 2, entry 5), thus suggesting a correlation between the relative acidities of the ammonium salt [36] and their catalytic activities. Additionally, NH<sub>4</sub>HSO<sub>4</sub> led to an almost quantitative conversion of **1a** to **3a** in the presence of 1.5–2.0 equivalents of **2a** (Table 2, entries 6 and 7), performing better in CPME than in toluene (Table 2, entry 7 versus entry 8). Interestingly, comparable results were obtained in the presence of a homogeneous acid catalyst, i.e., *p*-TSA (Table 2, entries 9 and 10). The above reported results could not be improved by employing Amberlyst 15<sup>®</sup> or Mont K10 as acidic catalysts (Table 2, entries 11 and 12) [37]. Indeed, although a relatively high conversion of the starting material was obtained with Amberlyst 15<sup>®</sup>, the reaction was accompanied by the formation of small amounts of unidentified by-products (Table 2, entry 11), whilst a poor conversion was obtained with Mont K10 (Table 2, entry 12).

Changing the solvent to 2-MeTHF and running the reactions in the presence of a catalytic amount of NH<sub>4</sub>HSO<sub>4</sub> led to poor conversions of **1a**, even in the presence of 2.0 equivalents of **2a** (Table 2, entries 13 and 14). Poorer results were obtained when employing Amberlyst 15<sup>®</sup> or Mont K10 as acidic catalysts (Table 2, entries 15 and 16). Possible rationalizations of these results can be found in both the different boiling points of the CPME/H<sub>2</sub>O versus 2-MeTHF/H<sub>2</sub>O azeotropic mixtures, and in the different removability of H<sub>2</sub>O from the reaction mixture by the different ethereal solvents (Table 1).

Finally, it is worth mentioning that both CPME and 2-MeTHF proved stable under these conditions, as established by the absence of any decomposition products within the reaction mixtures, as determined by <sup>1</sup>H-, <sup>13</sup>C-NMR and GLC analyses [38]. Accordingly, it was possible to realize an 80–85% mass recovery of both reaction solvents which were collected by evaporation of reaction mixtures, filtered over alumina, dried (KOH), and distilled. After stabilization with 2,6-di-*tert*-butyl-4-methylphenol (BHT), both solvents were successfully recycled to successive runs (Table 2, entries 7 and 14).

To assess the reusability of ammonium salts as acidic catalysts, selected reactions were submitted to a series of consecutive runs. After the end of each run, the reaction mixture was filtered and the recovered catalyst, washed on the filter with a few mL of the reaction solvent and dried in vacuo,

was reused for the next batch to find no significant loss of its catalytic activity (Table 2, entries 1–3, 5, and 7; for more details, see Table S1, Supplementary Materials).

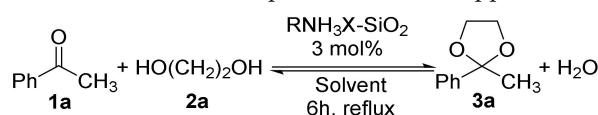
It should be emphasized, however, that the recovery of the catalyst from the reaction mixtures performed in the presence of excess diol was problematic due to the deliquescent texture they assume under these conditions, thus requiring their exhaustive washing with THF (Table 2, entries 6, 7, and 14).

To overcome this problem and to improve our protocol, we investigated the efficiency of several SiO<sub>2</sub>-supported ammonium salts (RNH<sub>3</sub>X-SiO<sub>2</sub>) as acidic catalysts.

To this end, 25% *w/w* dispersions of NH<sub>4</sub>HSO<sub>4</sub> and NH<sub>4</sub>Br and 17% *w/w* HCl.Gly on silica gel were prepared by wet impregnation and were successively employed as catalysts in our test reactions in CPME or 2-MeTHF [39].

Overall, the results in Table 3 show that the supported ammonium salts worked as efficient as their unsupported counterparts. Furthermore, they were particularly easy to handle and recover by filtration from reaction mixtures even in the presence of excess diol and were recycled without loss of their efficiencies (Table 3 entries 2–4; for more details, see Table S2, Supplementary Materials).

**Table 3.** Synthesis of dioxolane **3a** in the presence of SiO<sub>2</sub>-supported ammonium salts <sup>1</sup>.



Entry	2a (Equivalent)	Solvent	Catalyst	Product Distribution 1a/3a (%) <sup>2</sup>
1	1.1	CPME	NH <sub>4</sub> Br-SiO <sub>2</sub>	25/75
2	1.1	CPME	HCl.Gly-SiO <sub>2</sub>	35/65 <sup>3</sup>
3	1.1	CPME	NH <sub>4</sub> HSO <sub>4</sub> -SiO <sub>2</sub>	14/86 <sup>4</sup>
4	2.0	CPME	NH <sub>4</sub> HSO <sub>4</sub> -SiO <sub>2</sub>	<5/>95 <sup>4</sup>
5	1.1	CPME	SiO <sub>2</sub>	93/7
6	1.1	2-MeTHF	NH <sub>4</sub> HSO <sub>4</sub> -SiO <sub>2</sub>	51/49
7	2.0	2-MeTHF	NH <sub>4</sub> HSO <sub>4</sub> -SiO <sub>2</sub>	38/62

<sup>1</sup> All reactions were run at reflux for 6 h in the presence of 3 mol% of the catalyst, unless otherwise indicated;

<sup>2</sup> Determined by <sup>1</sup>H-NMR analyses of crude reaction mixtures; no other reaction products were detected;

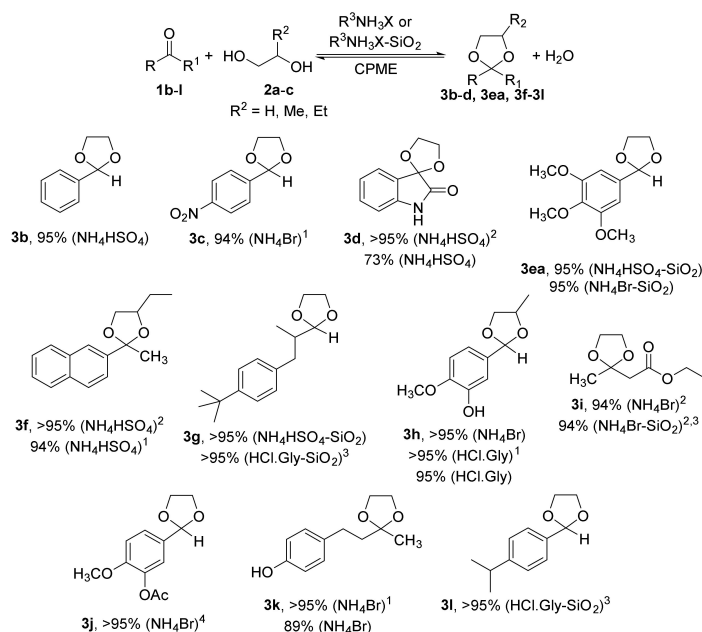
<sup>3</sup> Comparable results were obtained recycling the recovered catalyst twice; <sup>4</sup> Comparable results were obtained when recycling the recovered catalyst three times.

The effectiveness of our protocol was further confirmed by the synthesis of the series of acetals reported below (Schemes 1 and 2), thus expanding the scope of synthesized products reported in our previous communication (See Scheme SM1, Supplementary Materials).

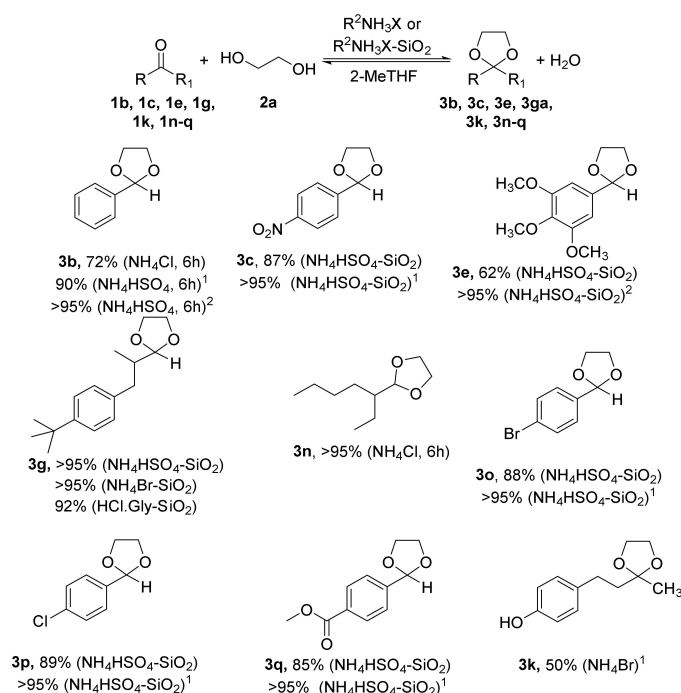
Scheme 1 shows new results performed in CPME leading, inter alia, to the synthesis of some known fragrances (**3f** [16], **3g** [40], **3h** [16,41], and **3i** [42]) or acetals of known fragrances (**3j** [43], **3k** [44], and **3l** [45]).

The reaction worked well with aliphatic and aromatic aldehydes in the presence of a minimal excess of diol (1.1–1.5 equivalent), whilst a relatively higher excess (1.5–2.0 equivalent) was required with less electrophilic ketones.

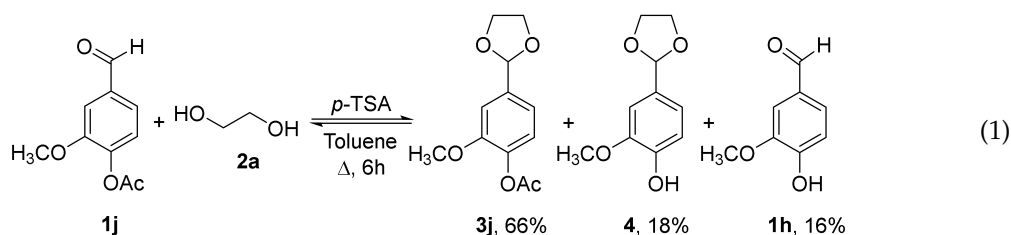
It is also worth noting that by employing NH<sub>4</sub>Br as a catalyst, it was possible to realize the synthesis of **3i** and **3j** in a chemoselective way, i.e., avoiding hydrolysis of the ester moieties, most likely due to the employment of a catalyst endowed with appropriate acidity [36]. Indeed, under similar conditions but employing NH<sub>4</sub>HSO<sub>4</sub> as an acidic catalyst, quantitative conversion of **1j** led to the formation of **3j** contaminated by trace amounts of **1h**, i.e., the product of acidic hydrolysis of the ester moiety of **1j** (not reported in Scheme 1). An even worse result was obtained when utilizing *p*-TSA, a stronger acid [46], as a catalyst and toluene as a solvent, as depicted in Equation (1). Under these conditions, 91% conversion of the starting material led to the formation of **3j**, **4** [47], and **1h** in a 66/18/16 ratio. In agreement with these findings, Corma et al. reported that the employment of strong acids and water formed during acetalization can cause the hydrolysis of the ester moiety of **1i/3i** [42].



**Scheme 1.** Synthesis of acetals in CPME. Reaction conditions: 4 M solution of **1** in CPME, 1.1 equivalent of **2a–c** (unless otherwise indicated), 3 mol% of  $\text{RNH}_3\text{X}$  or  $\text{RNH}_3\text{X-SiO}_2$  (with respect to **1**), reflux (Dean–Stark conditions). Percentages represent conversion of the starting materials as determined by  $^1\text{H-NMR}$ ; no other products, besides starting materials, were detected. <sup>1</sup> In the presence of 1.5 equivalent of diol; <sup>2</sup> In the presence of 2.0 equivalent of diol. <sup>3</sup> Comparable results were obtained recycling the recovered catalyst three times. <sup>4</sup> Isolated yield 78%, see Supplementary Materials.

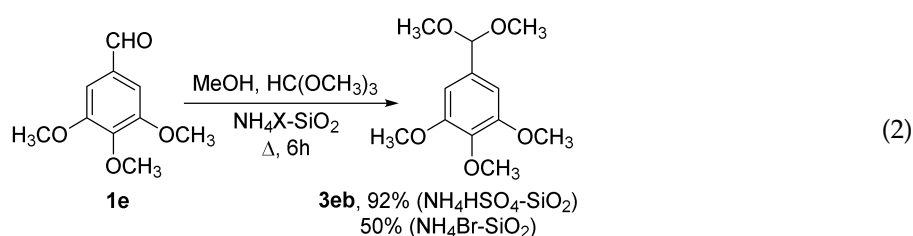


**Scheme 2.** Synthesis of acetals in 2-MeTHF. Reaction conditions: 4 M solution of **1** in CPME, 1.1 equivalent of **2a** (unless otherwise indicated), 3 mol% of  $\text{RNH}_3\text{X}$  or  $\text{RNH}_3\text{X-SiO}_2$  (with respect to **1**), reflux (Dean–Stark conditions). Percentages represent conversion of the starting materials as determined by  $^1\text{H-NMR}$ ; no other products, besides starting materials, were detected. <sup>1</sup> In the presence of 1.5 equivalent of diol; <sup>2</sup> In the presence of 2.0 equivalent of diol.

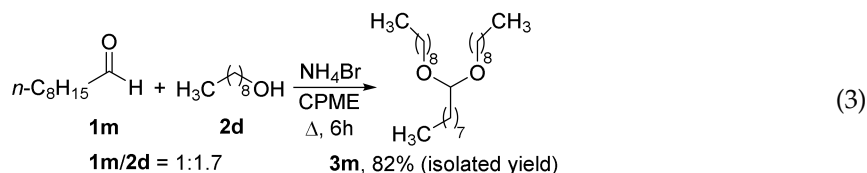


To widen the scope of our protocol, we slightly modified the above described experimental procedure to realize the synthesis of acetals of simple alcohols, such as methanol and nonanol.

Accordingly, we synthesized the dimethyl acetal of 3,4,5-trimethoxybenzaldehyde, **3eb**, by warming **1e** at 65 °C for 6 h with 1.1 equivalents of MeOH and 1.1 equivalents of HC(OCH<sub>3</sub>)<sub>3</sub> as a scavenger of water. Under the new conditions, the most acidic catalyst, i.e., NH<sub>4</sub>HSO<sub>4</sub>-SiO<sub>2</sub> proved more efficient as compared to NH<sub>4</sub>Br-SiO<sub>2</sub> (Equation (2)).



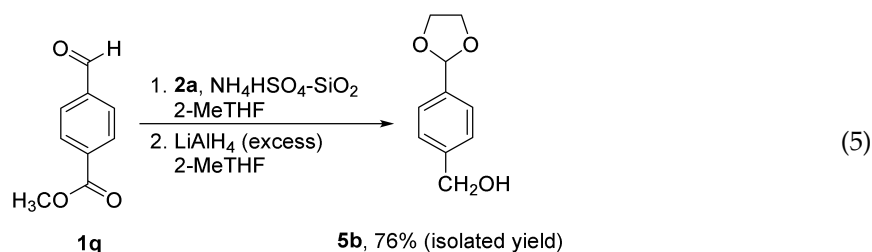
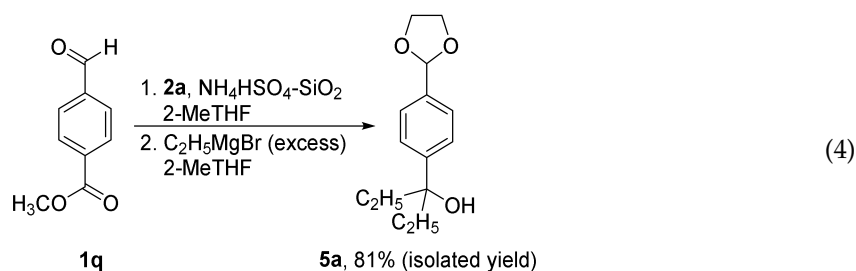
A good result was obtained in the synthesis of the dinonyl acetal of nonanal, **3m**, employing a lower than stoichiometric amount of **2d** to allow an easier separation of the reaction product from the unreacted starting material(s) by vacuum fractional distillation (Equation (3)).



An additional set of reactions was run by employing 2-MeTHF as a solvent (Scheme 2). Aliphatic aldehydes were almost completely converted into the corresponding acetals even in the presence of 1.1 equivalent of **2a** and of the relatively less acidic catalysts, HCl.Gly-SiO<sub>2</sub> or NH<sub>4</sub>Br-SiO<sub>2</sub> for the synthesis of **3g** or NH<sub>4</sub>Cl for the synthesis of **3n**.

At variance with these results, a higher excess of **2a** (1.5 to 2.0 equivalents) and the employment of NH<sub>4</sub>HSO<sub>4</sub> or NH<sub>4</sub>HSO<sub>4</sub>-SiO<sub>2</sub> as catalyst were required for the less electrophilic aromatic aldehydes **1b**, **1c**, **1e**, and **1o–q**. Poorer conversions were achieved with less electrophilic aromatic and aliphatic ketones such as **1k**, thus representing a limitation to the employment of 2-MeTHF as a solvent in the present methodology.

It is nonetheless worth noting that 2-MeTHF is particularly well suited for reactions involving highly polar nucleophilic reagents, such as organomagnesium [29,48,49] or organolithium compounds [29], i.e., for multistep reactions where the temporary protection of an aldehyde as an acetal is required. Accordingly, and in agreement with what already achieved for telescopic reactions run in CPME (see Equations (S1)–(S3) Supplementary Materials) [22], acetalization of **1q** followed by reaction of the crude acetal with excess ethylmagnesium bromide employing 2-MeTHF as a solvent under two-steps in one-pot reaction conditions, as depicted in Equation (4), led to the formation of the tertiary alcohol **5a** in 81% overall yield. Under related conditions, reduction in the crude acetal with LiAlH<sub>4</sub> afforded the corresponding benzyl alcohol, **5b**, in 76% overall yield (Equation (5)).



## 2.2. Preparation and Characterization of SiO<sub>2</sub>-Supported Ammonium Salts

SiO<sub>2</sub>-supported ammonium salts, namely NH<sub>4</sub>Br-SiO<sub>2</sub>, HCl.Gly-SiO<sub>2</sub>, and NH<sub>4</sub>HSO<sub>4</sub>-SiO<sub>2</sub> were prepared by wet impregnation [50]. The resulting products were characterized by means of Scanning Electron Microscopy (SEM), Transmission Electron Microscopy (TEM) coupled with energy-dispersive X-ray (EDX) spectroscopy, N<sub>2</sub> physisorption, and IR spectroscopy.

The microstructural, surface morphology, and elemental analysis of the samples were characterized by TEM and SEM. In Figure 1, representative SEM images of granular silica gel particles, after impregnation with the three above mentioned ammonium salts, are reported.

For all samples, the as-embedded silica particles are not regular in shape and are characterized experimentally by an average diameter of ca. 58 μm, in line with the dimension of the as-received SiO<sub>2</sub>.

Therefore, the treatment to which the raw silica particles are subjected appears to have an influence on their size and shape. Additionally, from the SEM images of surface, it is clear that the functionalized surface exhibits more roughness, with respect to the original (see Figure S1, Supplementary Materials), which is indicative of the anchoring ammonium salt components to the surface of silica gel.

To further confirm the effectiveness of the impregnation step, considering the amorphous nature of NH<sub>4</sub>HSO<sub>4</sub>-SiO<sub>2</sub> and HCl.Gly-SiO<sub>2</sub> provided by X-ray powder diffraction (see Figure S2, Supplementary Materials), FTIR was used to characterize the major chemical groups in the silica gel after impregnation. The FTIR spectra are depicted in Figure 2.

For all three samples, the characteristic and peak positions of the FTIR spectra of the as-modified silica gel match with those of commercial silica which was reported by Zhang and coauthors [51]. The broad peak centered at 3500 cm<sup>-1</sup> is due to the silanol OH group and the adsorbed water bonding to the silica surface by the hydrogen bond. The peaks at 1100, 800, and 490 cm<sup>-1</sup> can be assigned to asymmetric Si-O-Si stretching, symmetric Si-O-Si stretching, and to the O-Si-O bending vibrations, respectively (as example see Figure 2B).

All these peaks are common characteristics of the three samples analyzed, as better highlighted by the blue dashed lines in Figure 2. Additionally, the spectrum related to the sample NH<sub>4</sub>HSO<sub>4</sub>-SiO<sub>2</sub> (Figure 2A) presents four further signals, which can be associated with the vibrational modes of NH<sub>4</sub><sup>+</sup> (3170 and 1400 cm<sup>-1</sup>), HSO<sub>4</sub><sup>-</sup> (1190 cm<sup>-1</sup>), and SO<sub>4</sub><sup>2-</sup> (600 cm<sup>-1</sup>) species in NH<sub>4</sub>HSO<sub>4</sub>, as also reported in other studies [22,52–54].

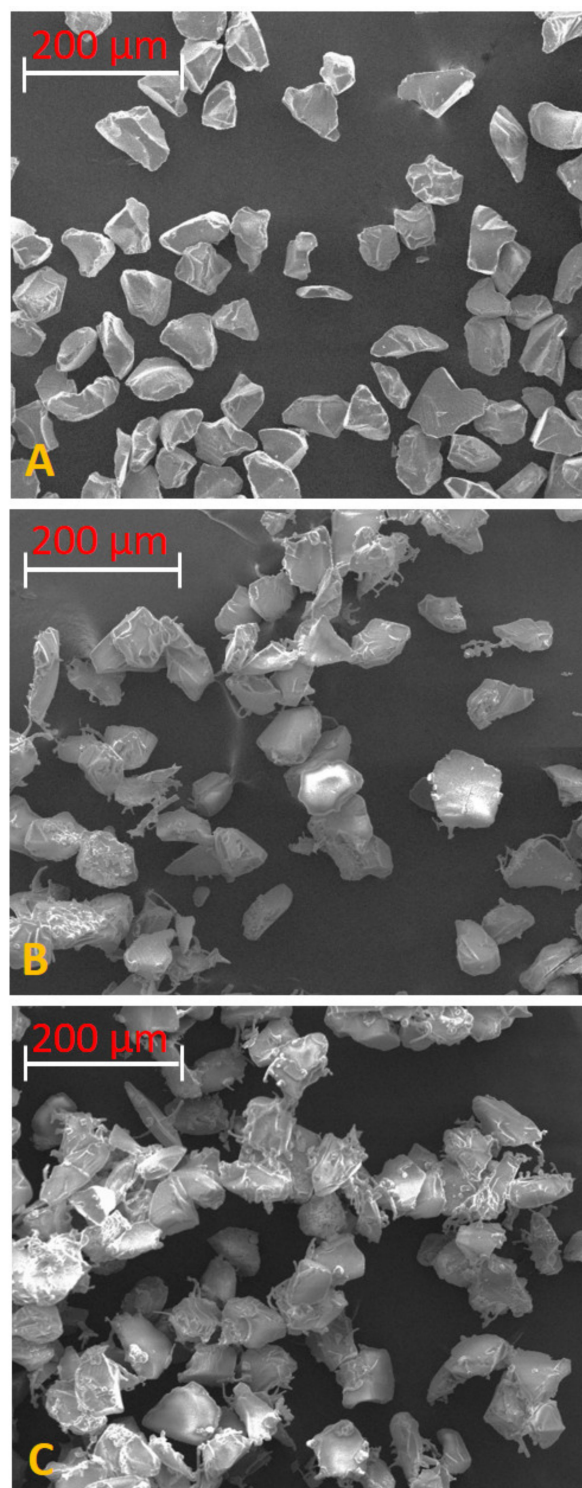


**Figure 1.** SEM image of silica gel beads impregnated with (A)  $\text{NH}_4\text{HSO}_4$ , (B)  $\text{HCl.Gly}$ , and (C)  $\text{NH}_4\text{Br}$ .

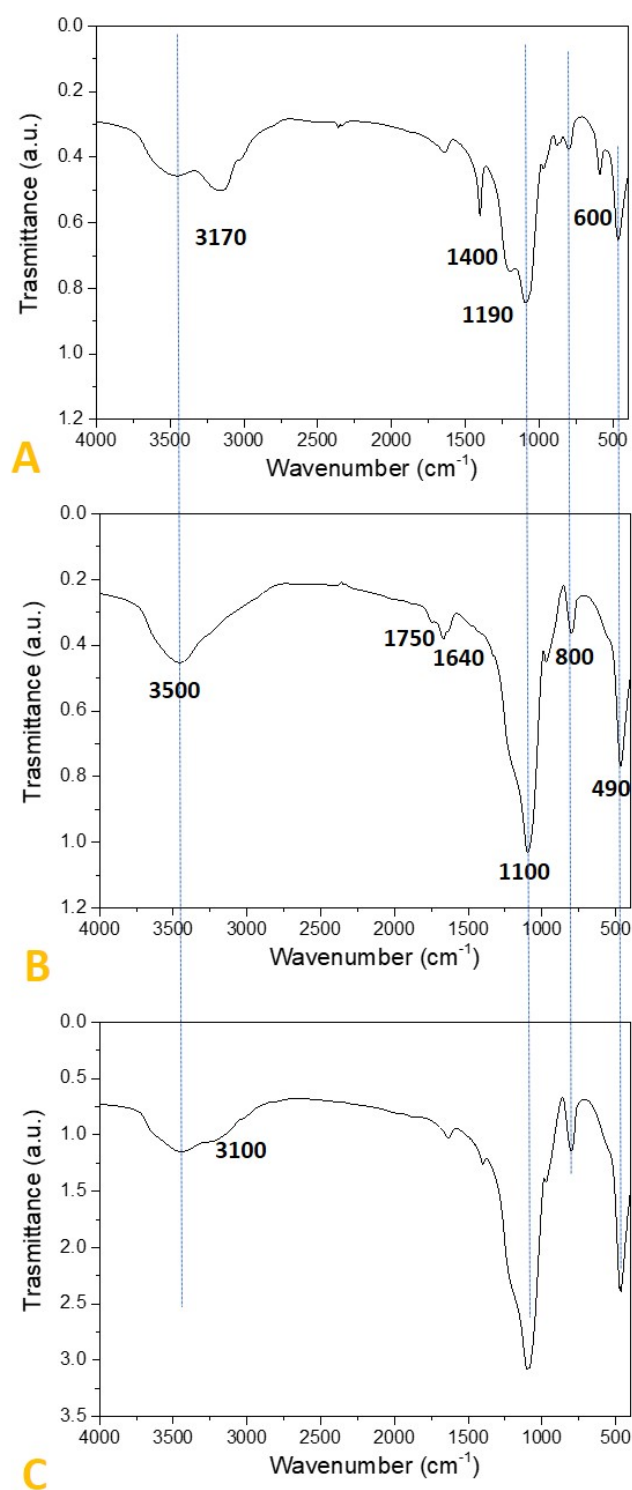


**Figure 2.** FTIR spectra of silica gel impregnated with (A)  $\text{NH}_4\text{HSO}_4$ , (B)  $\text{HCl.Gly}$ , and (C)  $\text{NH}_4\text{Br}$  ammonium salts.

Evidence of glycine hydrochloride ( $\text{HCl.Gly}$ ) has been confirmed by the characteristic peaks at 1750 and 1643  $\text{cm}^{-1}$  (Figure 2B) assigned to the CO stretch and  $\text{CO}_2$  asymmetric stretches, respectively [55]. The appearance of a new peak at 3100 in Figure 2C can be attributed to  $\text{NH}^+$  symmetric and asymmetric vibrations modes of  $\text{NH}_4\text{Br}$  [56]. It is also important that FTIR spectra, acquired after several catalytic

cycles, presented the same features reported in Figure 2. FTIR analysis performed on the exhausted solution, recovered after catalytic tests, did not reveal trace of ammonium salts.

In accordance with the high reproducibility of the catalytic performance as showed by these supported catalysts (see Table 3), this seems to confirm the effective immobilization of the ammonium salts on the SiO<sub>2</sub>.

Taking into consideration the nanoporous nature of SiO<sub>2</sub>, it should be clarified if the ammonium salts were immobilized on the surface and/or into the porous channels of SiO<sub>2</sub>. To shed light on this aspect, TEM characterization of the three samples was performed. Representative TEM micrographs of the as-prepared systems are shown in Figure 3.

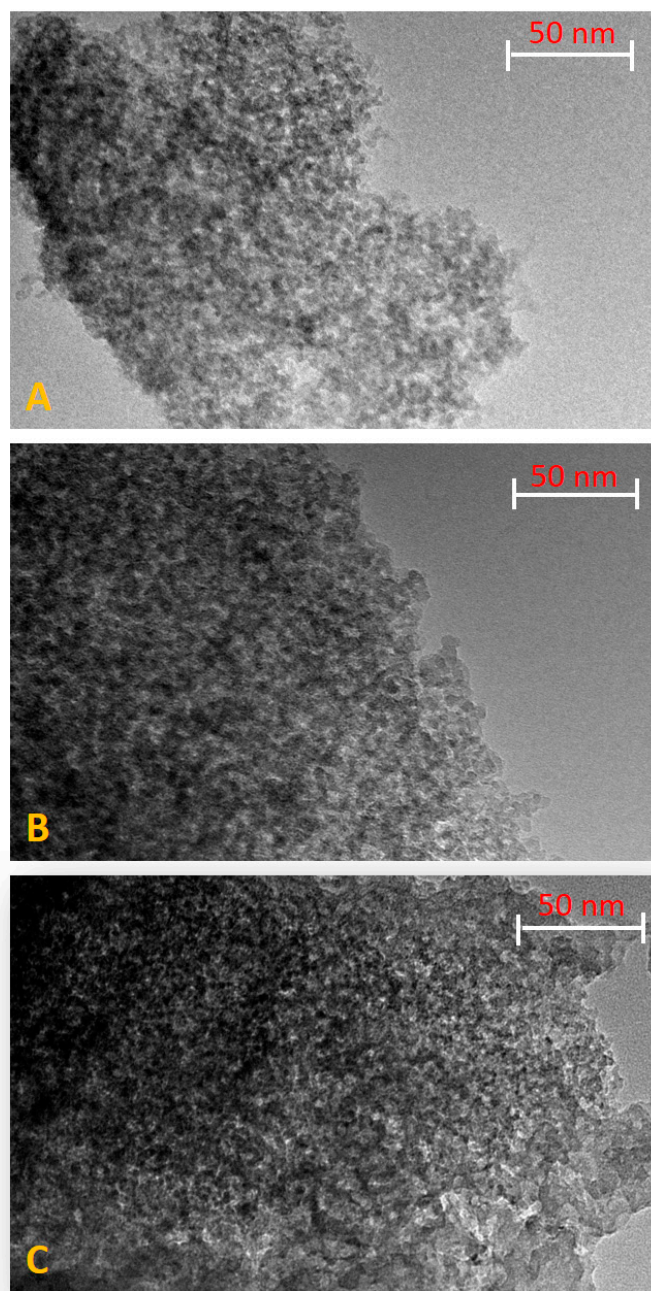


**Figure 3.** TEM spectra of the silica gel product impregnated with (A) NH<sub>4</sub>HSO<sub>4</sub>, (B) HCl.Gly, and (C) NH<sub>4</sub>Br.

As emerged from all the analysis, after the impregnation step, the porosity of the SiO<sub>2</sub> matrix is characterized by a larger distribution of porous diameter (4–9 nm) with respect to the untreated SiO<sub>2</sub>, while pore shape seems to be preserved. EDX analysis (see Figures S3–S5, Supplementary Materials) performed on the TEM images areas revealed that the specific elements, Cl, S, and Br, existed over a significant percentage, although light elements are difficult to quantify due to limited sensitivity. Furthermore, the presence of ammonium salts into the pores cannot be directly confirmed because they are characterized by low contrast with respect to the amorphous carbon support.

Specific surface area and pore distribution were calculated from N<sub>2</sub> sorption isotherms according to Brunauer, Emmett, and Teller (BET) and Barrett–Joyner–Halenda (BJH) approaches, respectively. N<sub>2</sub> physisorption isotherms and the pore size distribution plots of all the synthesized samples are depicted in Figure 4A–F.

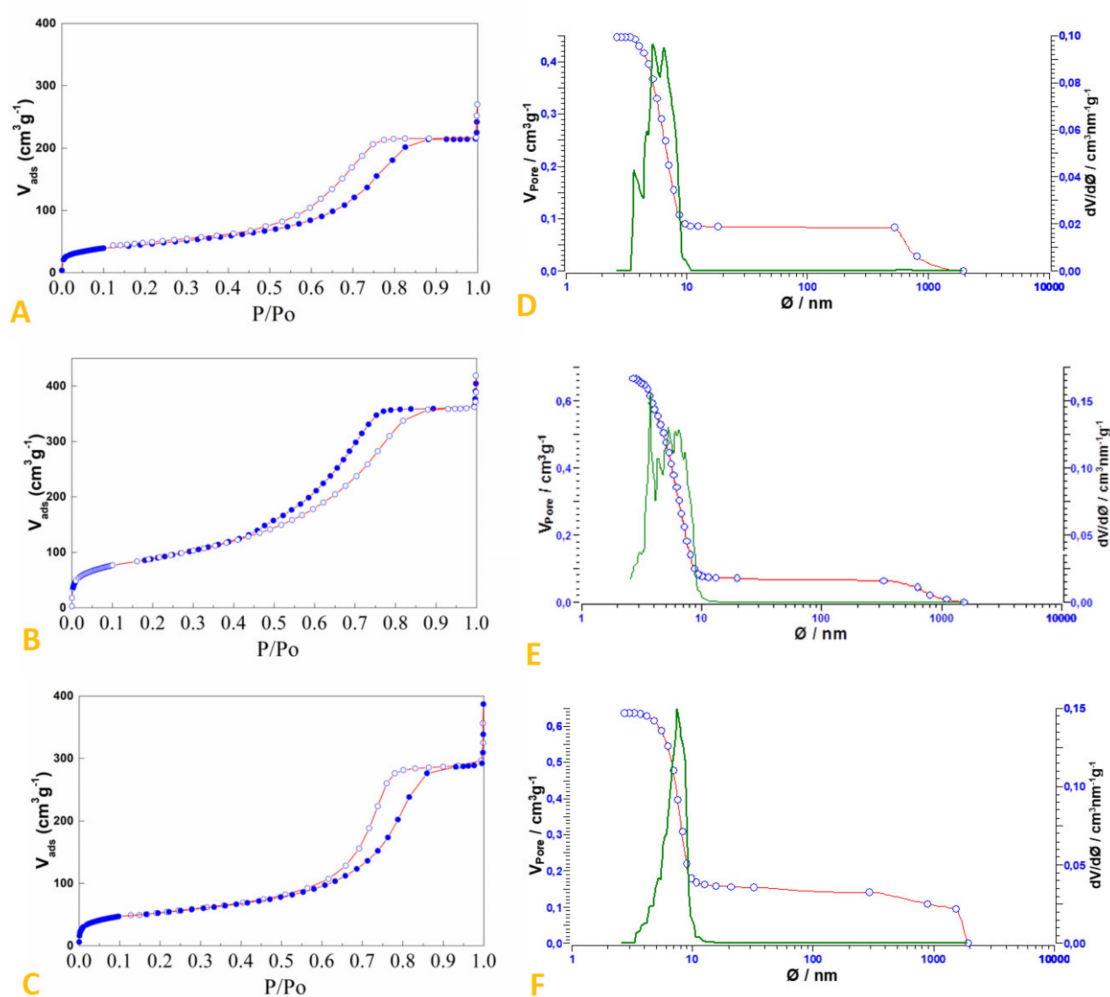


**Figure 4.** N<sub>2</sub> physisorption isotherms and the corresponding pore size distribution of (A), (D) NH<sub>4</sub>HSO<sub>4</sub>-SiO<sub>2</sub>, (B), (E) HCl.Gly-SiO<sub>2</sub> and (C), (F) NH<sub>4</sub>Br-SiO<sub>2</sub>.

BET surface areas vary from 161 to 185 m<sup>2</sup> g<sup>-1</sup> except for the sample impregnated with HCl.Gly, which exhibits a surface area of 319 m<sup>2</sup> g<sup>-1</sup> (see Table 4). All the samples show a type IV isotherm (Figure 4A–C) characteristic of mesoporous materials [57], in accordance with TEM analysis, with a H2(b) type hysteresis loop associated with pore blocking, typical of mesocellular silica foams and certain mesoporous ordered silicas [57,58]. The BJH pore size distributions of the impregnated SiO<sub>2</sub> matrices are illustrated in Figure 4D–F and show pores between 4 and 10 nm for all products.

**Table 4.** Parameters of porous structure of the as-prepared catalyst and commercial silica gel support.

System	Surface Area (m <sup>2</sup> /g)	Pore Volume (cm <sup>3</sup> /g)	Median Pore Width (nm)
Silica Gel (60 Å, 230–240 mesh)	550 <sup>1</sup>	≈0.8 <sup>1</sup>	6.0 <sup>1</sup>
HCl.Gly-SiO <sub>2</sub>	319	0.555	5.2
NH <sub>4</sub> Br-SiO <sub>2</sub>	185	0.444	5.5
NH <sub>4</sub> HSO <sub>4</sub> -SiO <sub>2</sub>	161	0.331	5.6

<sup>1</sup> Reference [59].

Nitrogen adsorption data are summarized in Table 4. The values of BET surface area, BJH average pore diameter, and cumulative volume of pores for silica gel decreased significantly for the three functionalized catalysts relative to the unreacted SiO<sub>2</sub> support, which can be ascribable to the fact that ammonium salts are present both on the surface and in the pores, as already suggested by SEM and TEM characterization.

### 2.3. Green Chemistry Metrics

Finally, in order to evaluate the sustainability of our procedure, we calculated and compared some green chemistry metrics for the synthesis of several acetals run with our green solvent/heterogeneous catalyst protocol with literature data for reactions run employing an aromatic solvent in the presence of *p*-TSA [60–65].

In addition to the reaction yield (better specified in Table 5), we chose to report Reaction Mass Efficiency (RME) [66] as a measure to show the usage of stoichiometric reactants and Process Mass Intensity (PMI) [67] to include the contribution of all materials used in the procedure. Indeed, PMI, is a metric of choice in industry because of its comprehensive nature and straightforward calculation [68,69]. The results, as reported in Table 5, concern the synthesis of acetals **3c**, **3d**, and **3o**, and the different methodologies employed in this work to synthesize acetal **3j**.

**Table 5.** Comparisons of green chemistry metrics for the synthesis of selected acetals.

Compound	Procedure [Ref]	Yield (%)	RME (%)	PMI
<b>3c</b>	This work	95 <sup>1</sup>	65	4.6
<b>3c</b>	Yang et al. [60]	100 <sup>1</sup>	70	20.5
<b>3c</b>	Wang et al. [61]	100 <sup>1</sup>	61	12.4
<b>3d</b>	This work	95 <sup>1</sup>	67	3.9
<b>3d</b>	Cliffe et al. [62]	99 <sup>2</sup>	48	63.4
<b>3d</b>	Wenkert et al. [63]	90 <sup>2</sup>	82	44.7
<b>3o</b>	This work	95 <sup>2</sup>	78	3.3
<b>3o</b>	Xu et al. [64]	100 <sup>2</sup>	28	37.4
<b>3o</b>	Nishi et al. [65]	95 <sup>2</sup>	25	20.4
<b>3j</b>	This work Toluene/ <i>p</i> -TSA	69 <sup>2</sup>	62	6.0
<b>3j</b>	This work CPME/NH <sub>4</sub> HSO <sub>4</sub>	63 <sup>2</sup>	57	3.2
<b>3j</b>	This work CPME/NH <sub>4</sub> Br	78 <sup>2</sup>	71	2.6

<sup>1</sup> Crude reaction product. <sup>2</sup> Purified by recrystallization.

Taken as a whole, RME values show how, with our procedure, the reactants are used with an efficiency that compares well with literature procedures, while PMI highlights the advantages due to the straightforward work-up and efficient use of solvents and catalysts of our protocol (for methods of calculations and additional information, see Supplementary Materials).

### 3. Materials and Methods

Starting materials, solvents and reagents were of the highest commercial quality and were employed as received, including silica gel (60 Å, 230–400 mesh) (Alfa Aesar, Kandel, Germany). FTIR and TEM characterization of commercial silica gel can be provided by the following manuscripts [70,71]. <sup>1</sup>H-NMR (400 MHz) and <sup>13</sup>C-NMR (100 MHz) spectra were recorded with a Ascend 400 spectrometer

(Bruker, Billerica, MA, USA) in  $\text{CDCl}_3$  (99.8% D content) solution with the residual peak of  $\text{CHCl}_3$  as the internal standard.  $\text{CDCl}_3$  was stored in a refrigerator under  $\text{K}_2\text{CO}_3$  to avoid deacetalization during spectra recording. FTIR spectra of reaction products were recorded from KBr pellets on a Fourier Transform Infrared Spectrophotometer FT/IR-480 Plus (Jasco, Tokyo, Japan). Gas chromatographic analyses were recorded on a 6890N Network GC System (Agilent, Santa Clara, CA, USA). The HRMS spectra were acquired on a Thermo Finnigan Q Exactive instrument (Thermo Instrument Systems Inc, Waltham, MA, USA) with an API-HESI source. Samples were introduced as 0.1 mg/L solutions in MS grade methanol with a 5  $\mu\text{L}/\text{min}$  flow and the following source parameters: positive polarity; sheath gas flow rate: 5 a.u.; aux gas flow rate: 3 a.u.; sweep gas flow rate: 0 a.u.; spray voltage: 3.50 kV; capillary temperature: 250  $^\circ\text{C}$ ; S-lens RF level: 60.0 V; aux gas heater temperature: 0  $^\circ\text{C}$ . The peroxide content of the solvents was tested employing semi-quantitative test-strips Quantofix<sup>®</sup> (Macherey-Nagel, Düren, Germany), measuring range 0.5–25 mg/L  $\text{H}_2\text{O}_2$ , in agreement with the general indications provided by the producer.

### 3.1. General Procedure for the Acetalization Reaction

In a 50 mL flask fitted with a Dean–Stark distiller and bubble condenser provided with a  $\text{CaCl}_2$  valve (for reactions in CPME or toluene) or under an Ar atmosphere (for reactions run in 2-MeTHF), the starting material (**1**, 80 mmol) was dissolved in the appropriate solvent (20 mL) together with the amount of the required diol (**2**, 88 to 160 mmol, 1.1 to 2.0 equivalent), as reported in Tables 2 and 3, Schemes 1 and 2, and Equations (1)–(5). After addition of the appropriate catalyst (2.4 mmol, 3 mol% of the starting material), the reaction mixture was heated in an oil bath under vigorous stirring and allowed to reflux for 6 h, then cooled to rt, and the reaction mixture was filtered. The reaction run in the presence of 1.5 to 2.0 equivalents of diol were then washed with  $\text{H}_2\text{O}$  ( $3 \times 5$  mL) and dried over anhydrous  $\text{Na}_2\text{SO}_4$ . The resulting solution was evaporated under reduced pressure and the crude product was analyzed by  $^1\text{H-NMR}$  spectroscopy. No other products, besides starting material, were detected, unless otherwise indicated (Tables 2 and 3, Schemes 1 and 2, and Equations (1)–(5)).

Recovery of the catalyst (washed twice with the reaction solvent and dried in vacuo) usually exceeded 90%.

Reaction products were identified by comparison with the literature data and/or with authentic samples synthesized according to the literature. For more details, see Supplementary Materials.

2-Methyl-2-phenyl-1,3-dioxolane, **3a**: Colorless oil, which solidifies upon standing; white crystals, mp 61–62  $^\circ\text{C}$  (CPME) [5c];  $^1\text{H NMR}$  (400 MHz,  $\text{CDCl}_3$ )  $\delta$  (ppm) 7.48 (2 H, d,  $J = 7.6$  Hz), 7.35 (2 H, t,  $J = 7.6$  Hz), 7.29 (2 H, t,  $J = 7.6$  Hz), 4.09–3.99 (m, 2 H), 3.83–3.73 (m, 2 H), 1.66 (3 H, s);  $^{13}\text{C NMR}$  ( $\text{CDCl}_3$ ; 100 MHz) = 143.2, 128.1, 127.8, 125.2, 108.8, 64.4, 27.6.

### 3.2. Preparation and Characterization of the $\text{SiO}_2$ -Supported Ammonium Salts

Silica-supported ammonium salts (25% *w/w* for  $\text{NH}_4\text{HSO}_4$  and  $\text{NH}_4\text{Br}$ , 17% for  $\text{HCl.Gly}$ ) were prepared by wet impregnation. A total of 20.0 g of  $\text{SiO}_2$  (column chromatographic grade, 60  $\text{Å}$ , 200–400 mesh) was added to a stirred solution of the appropriate amount of ammonium salt dissolved in 30 mL of  $\text{H}_2\text{O}$ . The resulting suspension was stirred at 50  $^\circ\text{C}$  for 1 h, followed by solvent evaporation under reduced pressure. The resulting white powder was dried at 120  $^\circ\text{C}$  for 48 h, then transferred and stored in a desiccator over anhydrous  $\text{CaCl}_2$ .

The microstructural, surface morphology, and elemental analysis of the samples were characterized by X-ray powder diffraction with a SmartLab diffractometer (Rigaku, Tokyo, Japan), transmission electron microscopy with a FEI TECNAI 200kV (Thermo Fisher Scientific, Waltham, MA, USA), and by scanning electron microscopy with a FEI QUANTA 200 (Thermo Fisher Scientific, Waltham, MA, USA). For TEM measurements, samples were prepared by dispersing a few milligrams in ethanol followed by the deposition of two drops of the suspension on an amorphous carbon-supported grid. For SEM imaging, a small amount of powder was deposited onto carbon tapes mounted on aluminum supports.

Fourier transform infrared spectroscopy (FTIR) measurements were performed with a FT/IR-480 Plus (Jasco, Tokyo, Japan) and all spectra were acquired with a resolution of  $1\text{ cm}^{-1}$ . Each sample (0.01 g) was finely mixed with ultra-dry KBr and pressed into pellets.

$\text{N}_2$  sorption isotherms were collected with a Sorptomatic 1990 instrument (Fisons Instruments, Thermo Instrument Systems Inc., Waltham, MA, USA) and the specific surface area and pore distribution were calculated according BET and BJH approaches, respectively. Before measurements, 200 mg of each sample were put in a quartz tube and degassed under dynamic vacuum ( $1 \times 10^{-3}$  bar) at 423 K for 24 h. The dead volume was evaluated through helium measurements.

#### 4. Conclusions

Our results underline the scope and limitations of an environmentally friendly protocol aimed at the acetalization of aldehydes and ketones in green ethereal solvents, namely CPME and 2-MeTHF, in the presence of ammonium salts as environmentally friendly, cheap, easily available, and relatively mild heterogeneous acidic catalysts.

Interestingly, whilst CPME efficiently promoted the acetalization of a wide array of aldehydes and ketones both with diols and, under appropriate conditions, with monohydric alcohols, reactions in 2-MeTHF led to satisfactory results only for the acetalization of aldehydes. Nonetheless, it is worth mentioning that, as already reported for CPME [22], 2-MeTHF effectively promoted multistep reactions, requiring the temporary protection of the aldehyde moiety towards strong nucleophilic reagents.

Both solvents proved stable under the reported conditions and their employment in the presence of heterogeneous catalysts allowed their easy recovery and recycling through an efficient work-up procedure, leading to a reduced amount of wastes.

In our test reactions, ammonium salts, either as such or supported on  $\text{SiO}_2$ , performed better or equally well of widely employed homogeneous and heterogeneous acidic catalysts such as *p*-TSA, Amberlyst 15<sup>®</sup>, or Mont K10. Several examples highlight the advantage of tuning the relative acidities of ammonium salts by appropriately selecting the counterion, as in the synthesis of compounds **3a**, **3eb**, **3i**, and **3j**. In the last example, the proposed ammonium salts/green ethereal solvent protocol clearly outweighed the classical *p*-TSA/toluene protocol in terms of chemoselectivity.

Furthermore, ammonium salts were easily recovered by filtration, particularly when supported on  $\text{SiO}_2$ , and recycled several times with no significant loss of their catalytic activities. Silica-supported catalysts were characterized by SEM, TEM, and FTIR spectroscopies, as well as by  $\text{N}_2$  physisorption, revealing an even distribution of HCl.Gly-OH,  $\text{NH}_4\text{Br}$ , and  $\text{NH}_4\text{HSO}_4$  on the silica, whilst EDX analyses display the presence of specific elements Cl, Br, and S, respectively, thus confirming the formation of the expected supported catalysts. Taken as a whole, the characterization results strongly suggest that ammonium salts are present both on the surface and in the pores of silica, thus providing supported catalysts endowed with relatively high stabilities.

**Supplementary Materials:** The following are available online at <http://www.mdpi.com/2073-4344/10/10/1108/s1>, General method, synthetic procedures, characterization data of all compounds including copies of  $^1\text{H}$  and  $^{13}\text{C}$  NMR spectra of previously not completely described compounds and of recycled solvents. Table S1: Performance of the recycled catalysts in the synthesis of dioxolane **3a**. Table S2: Performance of the recycled catalysts in the synthesis of dioxolane **3a** in the presence of  $\text{SiO}_2$ -supported ammonium salts. Figure S1: Representative SEM micrograph of the as-received  $\text{SiO}_2$  support. Figure S2: Wide-angle XRD patterns of the as-received  $\text{SiO}_2$ ,  $(\text{NH}_4)\text{HSO}_4$ , HCl Gly and  $\text{NH}_4\text{Br}$  supported systems. Figure S3: EDX spectrum of  $\text{NH}_4\text{HSO}_4\text{-SiO}_2$ . Figure S4: EDX spectrum of  $\text{NH}_4\text{Br-SiO}_2$ . Figure S5: EDX spectrum of HCl.Gly- $\text{SiO}_2$ . Green Metrics. Scheme SM1: Previous synthesis of acetals and amins in CPME. Equations (S1)–(S3): Two-step one-pot reactions in CPME. Literature references for the characterization of all reaction products. Literature references to Green Metrics.

**Author Contributions:** Conceptualization, U.A. and S.G. (Sebastano Garroni); formal analysis, U.A., M.C. (Massimo Carraro), S.G. (Sebastano Garroni) and N.S.; investigation: U.A., M.C. (Massimo Carraro), M.C. (Martina Corrias), R.C., S.G. (Sebastano Garroni), S.G. (Silvia Gaspa), L.D.L., L.N., L.P., S.P., R.P., M.S., G.S., and L.U.; methodology: U.A., M.C. (Massimo Carraro), S.G. (Sebastano Garroni) and N.S.; resources: U.A. and S.G. (Sebastano Garroni); supervision: U.A. and S.G. (Sebastano Garroni); writing—original draft: U.A., M.C. (Massimo Carraro), S.G. (Sebastano Garroni), G.S. and N.S. All authors have read and agreed to the published version of the manuscript.

**Funding:** U.A., M.C. (Massimo Carraro) and S.G. (Sebastiano Garroni) acknowledge UNISS for the financial support received within the program “Fondo di Ateneo per la ricerca 2019”.

**Acknowledgments:** We thank Zeon Corporation for the gift of a generous sample of CPME through their Italian retailer IMCD Italia SpA. We acknowledge the CeSAR (Centro Servizi d’Ateneo per la Ricerca) of the University of Sassari for the HRMS, scanning and transmission electron microscopy analysis.

**Conflicts of Interest:** The authors declare no conflict of interest.

## References and Notes

1. Prat, D.; Wells, A.; Hayler, J.; Sneddon, H.; McElroy, C.R.; Abou-Shehadeh, S.; Dunne, P.J. CHEM21 selection guide of classical- and less classical-solvents. *Green Chem.* **2016**, *18*, 288–296. [[CrossRef](#)]
2. Henderson, R.K.; Jiménez-González, C.; Constable, D.J.C.; Alston, S.R.; Inglis, G.G.A.; Fisher, G.; Sherwood, J.; Binks, S.P.; Curzons, A.D. Expanding GSK’s solvent selection guide—Embedding sustainability into solvent selection starting at medicinal chemistry. *Green Chem.* **2011**, *13*, 854–862. [[CrossRef](#)]
3. Raymond, M.J.; Slater, C.S.; Savelski, M.J. LCA approach to the analysis of solvent waste issues in the pharmaceutical industry. *Green Chem.* **2010**, *12*, 1826–1834. [[CrossRef](#)]
4. Alfonsi, K.; Colberg, J.; Dunn, P.J.; Fevig, T.; Jennings, S.; Johnson, T.A.; Kleine, H.P.; Knight, C.; Nagy, M.A.; Perry, D.A.; et al. Green chemistry tools to influence a medicinal chemistry and research chemistry based organisation. *Green Chem.* **2008**, *10*, 31–36. [[CrossRef](#)]
5. Capello, C.; Fischer, U.; Hungerbühler, K. What is a green solvent? A comprehensive framework for the environmental assessment of solvents. *Green Chem.* **2007**, *9*, 927–934. [[CrossRef](#)]
6. Sheldon, R.A. Green solvents for sustainable organic synthesis: State of the art. *Green Chem.* **2005**, *7*, 267–272. [[CrossRef](#)]
7. Surburg, H.; Panten, J. *Common Fragrance and Flavour Materials*, 5th ed.; Wiley VCH: Weinheim, Germany, 2006; pp. 12–17, 38–44, 111–119.
8. Hermann, A. Profragrances and properfumes. In *The Chemistry and Biology of Volatiles*; Hermann, A., Ed.; Wiley: Chichester, UK, 2010; pp. 333–362.
9. Sivik, M.R. Profragrance Cyclic Acetals. WO Patent 99/00377, 26 June 1998.
10. de Carvalho, D.C.; Oliveira, A.C.; Ferreira, O.P.; Filho, J.M.; Tehuacanero-Cuapa, S.; Oliveira, A.C. Titanate nanotubes as acid catalysts for acetalization of glycerol with acetone: Influence of the synthesis time and the role of structure on the catalytic performance. *Chem. Eng. J.* **2017**, *313*, 1454–1467. [[CrossRef](#)]
11. Zhang, F.; Jin, Y.; Shi, J.; Zhong, Y.; Zhu, W.; El-Shall, M.S. Polyoxometalates confined in the mesoporous cages of metal–organic framework MIL-100(Fe): Efficient heterogeneous catalysts for esterification and acetalization reactions. *Chem. Eng. J.* **2015**, *269*, 236–244. [[CrossRef](#)]
12. Gonzalez-Arellano, C.; Deb, S.; Luque, R. Selective glycerol transformations to high value-added products catalysed by aluminosilicate-supported iron oxide nanoparticles. *Catal. Sci. Technol.* **2014**, *4*, 4242–4249. [[CrossRef](#)]
13. Malleshham, B.; Sudarsanam, P.; Raju, G.; Reddy, B.M. Design of highly efficient Mo and W-promoted SnO<sub>2</sub> solid acids for heterogeneous catalysis: Acetalization of bio-glycerol. *Green. Chem.* **2013**, *15*, 478–489. [[CrossRef](#)]
14. Miao, J.; Wan, H.; Shao, Y.; Guan, G.; Xu, B. Acetalization of carbonyl compounds catalyzed by acidic ionic liquid immobilized on silica gel. *J. Mol. Cat. A Chem.* **2011**, *348*, 77–82. [[CrossRef](#)]
15. Deutsch, J.; Martin, A.; Lieske, H. Investigations on heterogeneously catalysed condensations of glycerol to cyclic acetals. *J. Catal.* **2007**, *245*, 428–435. [[CrossRef](#)]
16. Climent, M.J.; Corma, A.; Velty, A. Synthesis of hyacinth, vanilla, and blossom orange fragrances: The benefit of using zeolites and delaminated zeolites as catalysts. *Appl. Catal. A Gen.* **2004**, *263*, 155–161, and references therein. [[CrossRef](#)]
17. Sartori, G.; Ballini, R.; Bigi, R.; Bosica, G.; Maggi, R.; Righi, P. Protection (and deprotection) of functional groups in organic synthesis by heterogeneous catalysis. *Chem. Rev.* **2004**, *104*, 199–250. [[CrossRef](#)]
18. Palaniappan, S.; Narander, P.; Saravanan, C.; Rao, V.J. Polyaniline-supported sulfuric acid salt as a powerful catalyst for the protection and deprotection of carbonyl compounds. *Synlett* **2003**, 1793–1796. [[CrossRef](#)]
19. Green, T.W.; Wuts, P.G.M. Protection of the carbonyl group. In *Protective Groups in Organic Synthesis*, 3rd ed.; Wiley: New York, NY, USA, 1999; pp. 293–329.

20. Azzena, U.; Carraro, M.; Modugno, G.; Pisano, L.; Urtis, L. Heterogeneous acidic catalysts for the tetrahydropyranylation of alcohols and phenols in green ethereal solvents. *Beilstein J. Org. Chem.* **2018**, *14*, 1655–1659. [[CrossRef](#)]
21. Azzena, U. 1,2-Diaryl-1,2-disodioethanes—Versatile, highly reactive, and tunable synthetic equivalents of sodium metal. *Aust. J. Chem.* **2017**, *70*, 647–651. [[CrossRef](#)]
22. Azzena, U.; Carraro, M.; Mamuye, A.D.; Murgia, I.; Pisano, L.; Zedde, G. Cyclopentyl methyl ether-NH<sub>4</sub>X—A novel solvent—Catalyst system for low impact acetalization reactions. *Green Chem.* **2015**, *17*, 3281–3284. [[CrossRef](#)]
23. Azzena, U.; Kondrot, F.; Pisano, L.; Pittalis, M. A green solvent approach to the chemistry of 1,2-Diaryl-1,2-disodioethanes. *Appl. Organometal. Chem.* **2012**, *26*, 180–184. [[CrossRef](#)]
24. Watanabe, K.; Yamagiwa, N.; Torisawa, Y. Cyclopentyl methyl ether as a new and alternative process solvent. *Org. Proc. Res. Dev.* **2007**, *11*, 251–258. [[CrossRef](#)]
25. Sakamoto, S. Contribution of cyclopentyl methyl ether (CPME) to green chemistry. *Chim. Oggi* **2013**, *31*, 24–27.
26. Azzena, U.; Carraro, M.; Pisano, L.; Monticelli, S.; Bartolotta, R.; Pace, V. Cyclopentyl methyl ether—An elective eco-friendly ethereal solvent in classical and modern organic chemistry. *ChemSusChem* **2019**, *12*, 40–70. [[CrossRef](#)]
27. de Gonzalo, G.; Alcántara, A.R.; Dominguez de María, P. Cyclopentyl methyl ether (CPME): A versatile eco-friendly solvent for applications in biotechnology and biorefineries. *ChemSusChem* **2019**, *12*, 2083–2097. [[CrossRef](#)]
28. Alcántara, A.R.; Domínguez de María, P. Recent advances on the use of 2-methyltetrahydrofuran (2-MeTHF) in biotransformations. *Curr. Green Chem.* **2018**, *5*, 86–103. [[CrossRef](#)]
29. Monticelli, S.; Castoldi, L.; Murgia, I.; Senatore, R.; Mazzeo, E.; Wackerlig, J.; Urban, E.; Langer, T.; Pace, V. Recent advancements on the use of 2-methyltetrahydrofuran in organometallic chemistry. *Monatsch. Chem.* **2017**, *148*, 37–48. [[CrossRef](#)]
30. Pace, V.; Hoyos, P.; Castoldi, L.; Dominguez de María, P.; Alcántara, A.R. 2-methyltetrahydrofuran (2-MeTHF): A biomass-derived solvent with broad application in organic chemistry. *ChemSusChem* **2012**, *5*, 1369–1379. [[CrossRef](#)]
31. Aycok, D.F. Solvent applications of 2-methyltetrahydrofuran in organometallic and biphasic reactions. *Org. Proc. Res. Dev.* **2007**, *11*, 156–159. [[CrossRef](#)]
32. *Handbook of Chemistry and Physics*, 57th ed.; Weast, R.C. (Ed.) CRC Press: Cleveland, OH, USA, 1976–1977; pp. D 1–D 36.
33. Watanabe, K. The toxicological assessment of cyclopentyl methyl ether (CPME) as a green solvent. *Molecules* **2013**, *18*, 3183–3194. [[CrossRef](#)]
34. Antonucci, V.; Coleman, J.; Ferry, J.B.; Johnson, N.; Mathe, M.; Scott, J.P.; Xu, J. Toxicological assessment of 2-methyltetrahydrofuran and cyclopentyl methyl ether in support of their use in pharmaceutical chemical process development. *Org. Proc. Res. Dev.* **2011**, *15*, 939–941. [[CrossRef](#)]
35. No conversion of the starting material was observed in the presence of 3 mol% of glycine.
36. pK<sub>a</sub> (in H<sub>2</sub>O): HSO<sub>4</sub><sup>−</sup> = 1.99 and NH<sub>4</sub><sup>+</sup> = 9.25: *Lange's Handbook of Chemistry*, 15th ed.; Dean, J.A. (Ed.) McGraw-Hill: New York, NY, USA, 1999; Table 8.7.
37. Poor conversions have already been observed for reactions run in the presence of (unactivated) zeolite ZSM-5 or (activated) molecular sieves (3 Å); see ref. [22].
38. As a note of caution, it is worth noting that reactions run under atmospheric conditions (CaCl<sub>2</sub> valve) in 2-MeTHF (see Experimental Part and Supplementary Materials) led to the formation of minor amounts of peroxides (<5 mg/L) as semiquantitatively evaluated with a commercially available kit (Quantofix®, measuring range 05–25 mgL<sup>−1</sup> H<sub>2</sub>O<sub>2</sub>). Indeed, the degradation mechanism of 2-MeTHF under free radical conditions, involving peroxide intermediates, was recently reported: Kobayashi, S.; Tamura, T.; Yoshimoto, S.; Kawakami, T.; Masuyama, A. 4-Methyltetrahydropyran (4-MeTHP): Application as an Organic Reaction Solvent. *Chem. Asian J.* **2019**, *14*, 3921–3937, Accordingly, such reactions can be more safely run under an inert atmosphere.

39. For a solvent free SiO<sub>2</sub> mediated synthesis of acetals under autogenous pressure, see: Rohand, T.; Savary, J.; Markó, I.E. Synthesis of dioxolanes and oxazolidines by silica gel catalysis. *Monatsh. Chem.* **2018**, *149*, 1429–1436.
40. Vyglazov, O.G.; Chuiko, V.A.; Izotova, L.V.; Vintarskaya, Z.V.; Yudenko, R.Y. Synthesis and perfume characteristics of acetals containing an aromatic ring. *Russ. J. Appl. Chem.* **2001**, *74*, 1888–1891. [[CrossRef](#)]
41. Kenya, I.; Takashi, A. Vanillin Acetals and Sensory Stimulation Composition Containing the Same. WO Patent 2007004740 (A1), 1 January 2007.
42. Clement, M.J.; Corma, A.; Velty, A.; Susarte, M. Zeolites for the production of fine chemicals: Synthesis of the fructose fragrance. *J. Catal.* **2000**, *196*, 345–351. [[CrossRef](#)]
43. Perflavory. Available online: <http://www.perflavory.com/docs/doc1035181.html> (accessed on 31 August 2020).
44. Perflavory. Available online: <http://www.perflavory.com/docs/doc1020771.html> (accessed on 31 August 2020).
45. The Good Scents Company Information System. Available online: <http://www.thegoodscentscompany.com/data/rw1004031.html> (accessed on 31 August 2020).
46. *pKa* (in H<sub>2</sub>O): P-TSA = −1.34: Serjeant, E.P.; Dempsey, B. *Ionisation Constants of Organic Acids in Aqueous Solution*; IUPAC Chemical Data Series No 23; Pergamon Press: New York, NY, USA, 1979.
47. Harrowven, D.C.; Woodcock, T.; Howes, P.D. Total synthesis of cavicularin and riccardin C: Addressing the synthesis of an arene that adopts a boat configuration. *Angew. Chem. Int. Ed.* **2005**, *44*, 3899–3901. [[CrossRef](#)]
48. Kadam, A.; Nguyen, M.; Kopach, M.; Richardson, P.; Gallou, F.; Wan, Z.-K.; Zhang, W. Comparative performance evaluation and systematic screening of solvents in a range of Grignard reactions. *Green Chem.* **2013**, *15*, 1880–1888. [[CrossRef](#)]
49. For an in-deep investigation on the reactivity of Grignard reagents in CPME, see: Kobayashi, S.; Shibukawa, K.; Miyaguchi, Y.; Masuyama, A. Grignard reactions in cyclopentyl methyl ether. *Asian J. Org. Chem.* **2016**, *5*, 636–645. [[CrossRef](#)]
50. Breton, G.W. Selective monoacetylation of unsymmetrical diols catalyzed by silica gel-supported sodium hydrogen sulfate. *J. Org. Chem.* **1997**, *62*, 8952–8954. [[CrossRef](#)]
51. Cui, Y.; Bu, X.; Zou, H.; Xu, X.; Zhou, D.; Liu, H.; Zhang, X.; Liu, Y.; Sun, H.; Jiang, J.; et al. A dual solvent evaporation route for preserving carbon nanoparticle fluorescence in silica gel and producing white light-emitting diodes. *Mater. Chem. Front.* **2017**, *1*, 387–393. [[CrossRef](#)]
52. Shi, Y.-J.; Shu, H.; Zhang, Y.-H.; Fan, H.-M.; Zhang, Y.-P.; Yang, L.-J. Formation and decomposition of NH<sub>4</sub>HSO<sub>4</sub> during selective catalytic reduction of NO with NH<sub>3</sub> over V<sub>2</sub>O<sub>5</sub>-WO<sub>3</sub>/TiO<sub>2</sub> catalysts. *Fuel Process. Technol.* **2016**, *150*, 141–147. [[CrossRef](#)]
53. Cziczó, D.J.; Abbatt, J.P.D. Infrared observations of the response of NaCl, MgCl<sub>2</sub>, NH<sub>4</sub>HSO<sub>4</sub>, and NH<sub>4</sub>NO<sub>3</sub> aerosols to changes in relative humidity from 298 to 238 K. *J. Phys. Chem. A* **2000**, *104*, 2038–2047. [[CrossRef](#)]
54. Ye, D.; Qu, R.; Liu, S.; Zheng, C.; Gao, X. New insights into the decomposition behavior of NH<sub>4</sub>HSO<sub>4</sub> on the SiO<sub>2</sub>-decorated SCR catalyst and its enhanced SO<sub>2</sub>-resistant ability. *ACS Omega* **2019**, *4*, 4927–4935. [[CrossRef](#)]
55. Fischer, G.; Cao, X.; Cox, N.; Francis, M. The FT-IR spectra of glycine and glycylglycine zwitterions isolated in alkali halide matrices. *Chem. Phys.* **2005**, *313*, 39–49. [[CrossRef](#)]
56. Shukur, M.F.; Kadir, M.F.Z. Electrical and transport properties of NH<sub>4</sub>Br-doped cornstarch-based solid biopolymer electrolyte. *Ionics* **2015**, *21*, 111–124. [[CrossRef](#)]
57. Sing, K.S.W.; Everett, D.H.; Haul, R.A.W.; Moscou, L.; Pierotti, R.A.; Rouquéro, J.; Siemieniowska, T. Reporting physisorption data for gas/solid systems with special reference to the determination of surface area and porosity. *Pure Appl. Chem.* **1985**, *57*, 603–619. [[CrossRef](#)]
58. Liu, W.; Yin, P.; Liu, X.; Dong, X.; Zhang, J.; Xu, Q. Thermodynamics, kinetics, and isotherms studies for gold(III) adsorption using silica functionalized by diethylenetriaminemethylenephosphonic acid. *Chem. Eng. Res. Des.* **2013**, *91*, 2748–2758. [[CrossRef](#)]
59. Sigma-Aldrich. Available online: <https://www.sigmaaldrich.com/catalog/product/sial/227196?lang=it&region=IT>, (accessed on 31 August 2020).
60. Yang, T.; Liu, Q.; Cheng, Y.; Cai, W.; Ma, Y.; Yang, L.; Wu, Q.; Orband-Miller, L.A.; Zhou, L.; Xiang, Z.; et al. Discovery of tertiary amine and indole derivatives as potent ROR $\gamma$ t inverse agonists. *ACS Med. Chem. Lett.* **2014**, *5*, 65–68. [[CrossRef](#)] [[PubMed](#)]
61. Wang, Y.; Qiu, R.; Gong, J.; Tian, J.; Huang, Y. Tertiary Amine Derivative or Salt Thereof, Preparation Method and Application Thereof. CN Patent CN109206346 (A), 20 December 2019. The experimental procedure in English is reported in Reaxys®.

62. Cliffe, I.A.; Lien, E.L.; Mansell, H.L.; Steiner, K.E.; Todd, R.S.; White, A.C.; Black, R.M. Oral hypoglycemic agents. Pyrimido [1,2-a]indoles and related compounds. *J. Med. Chem.* **1992**, *35*, 1169–1175. [[CrossRef](#)]
63. Wenkert, E.; Hudlický, T. Reactions of isatin dimethyl ketal and its ethyl imino ether with methyllithium. *Synth. Commun.* **1977**, *7*, 541–547. [[CrossRef](#)]
64. Xu, G.; Lei, H.; Zhou, G.; Zhang, C.; Xie, L.; Zhang, W.; Cao, R. Boosting hydrogen evolution by using covalent frameworks of fluorinated cobalt porphyrins supported on carbon nanotubes. *Chem. Commun.* **2019**, *55*, 12647–12650. [[CrossRef](#)]
65. Nishi, H.; Namari, T.; Kobatake, S. Photochromic polymers bearing various diarylethene chromophores as the pendant: Synthesis, optical properties, and multicolor photochromism. *J. Mater. Chem.* **2011**, *21*, 17249–17258. [[CrossRef](#)]
66. Curzons, A.D.; Constable, D.J.C.; Mortimer, D.N.; Cunningham, V.L. So you think your process is green, how do you know?—Using principles of sustainability to determine what is green—A corporate perspective. *Green Chem.* **2001**, *3*, 1–6. [[CrossRef](#)]
67. Jiménez-González, C.; Ponder, C.S.; Broxterman, Q.B.; Manley, J.B. Using the right green yardstick: Why process mass intensity is used in the pharmaceutical industry to drive more sustainable processes. *Org. Process Res. Dev.* **2011**, *15*, 912–917. [[CrossRef](#)]
68. Li, J.; Simmons, E.M.; Eastgate, M.D. A data-driven strategy for predicting greenness scores, rationally comparing synthetic routes and benchmarking PMI outcomes for the synthesis of molecules in the pharmaceutical industry. *Green Chem.* **2017**, *19*, 127–139. [[CrossRef](#)]
69. Andraos, J. Critical evaluation of published algorithms for determining material efficiency green metrics of chemical reactions and synthesis plans. *ACS Sustain. Chem. Eng.* **2016**, *4*, 1917–1933. [[CrossRef](#)]
70. Radi, S.; Basbas, N.; Tighadouini, S.; Bacquet, M. New polysiloxane surfaces modified with ortho-, meta- or para-nitrophenyl receptors for copper adsorption. *J. Surf. Eng. Mater. Adv. Technol.* **2014**, *4*, 21–28.
71. Burhan, M.; Shahzad, M.W.; Ng, K.C. A universal theoretical framework in material characterization for tailored porous surface design. *Sci. Rep.* **2019**, *9*, 8773. [[CrossRef](#)]



© 2020 by the authors. Licensee MDPI, Basel, Switzerland. This article is an open access article distributed under the terms and conditions of the Creative Commons Attribution (CC BY) license (<http://creativecommons.org/licenses/by/4.0/>).